

Simulation of Combustion Field with Lattice Boltzmann Method

Kazuhiro Yamamoto ^{1,2}, Xiaoyi He ², and Gary D. Doolen ²

¹ *Mechanical Engineering, Toyohashi University of Technology
1-1 Tempaku, Hibarigaoka, Toyohashi, Aichi 441-8580, Japan*

² *Theoretical Division, Los Alamos National Laboratory
Los Alamos, New Mexico 87545, U.S.A.*

(Abstract)

Turbulent combustion is ubiquitously used in practical combustion devices. However, even chemically non-reacting turbulent flows are complex phenomena, and chemical reactions make the problem even more complicated. Due to the limitation of the computational costs, conventional numerical methods are impractical in carrying out direct 3D numerical simulations at high Reynolds numbers with detailed chemistry. Recently, the lattice Boltzmann method has emerged as an efficient alternative for numerical simulation of complex flows. Compared with conventional methods, the lattice Boltzmann scheme is simple and easy for parallel computing. In this study, we present a lattice Boltzmann model for simulation of combustion, which includes reaction, diffusion, and convection. We assume the chemical reaction does not affect the flow field. Flow, temperature, and concentration fields are decoupled and solved separately. As a preliminary simulation, we study the so-called "counter-flow" laminar flame. The particular flow geometry has two opposed uniform combustible jets which form a stagnation flow. The results are compared with those obtained from solving Navier-Stokes equations.

INTRODUCTION

Turbulent combustion is present in most combustion devices. Under practical conditions, turbulence is a complex three-dimensional phenomenon. In combustion processes, many reactions between stable species and radicals occur [1,2]. These chain reactions consist of a series of consecutive, competitive, and opposing reactions with different reaction rate constants. These chemical reactions make the problem quite more complicated, and it is often crucial to include the detailed chemistry and the three-dimensional behavior of turbulent combustion. Due to the limitation of the computational costs, conventional numerical methods are impractical in carrying out direct numerical simulations.

Recently, the lattice Boltzmann method (LBM) has emerged as an efficient alternative for numerical simulation [3]. For example, He and Doolen have simulated the flow around two-dimensional circular cylinder to show the time evolution of vortex shedding [4]. Martinez et al. have examined the turbulence in shear layer, and the turbulence flow can be well simulated at a relatively high Reynolds number of 10,000 [5]. Compared with conventional methods, the lattice Boltzmann scheme is simple and easy for parallel computing. It has been used for direct numerical simulation (DNS). Therefore, combustion field can be simulated if the reaction term is well described.

The reactive flow has been simulated in several studies by using LBM. For example, Chen et al. have examined the effect of fluid flow on chemical reaction on solid surfaces to study geochemical process including dissolution and precipitation [6]. Recently, some groups have tried combustion problem using special treatment for chemical reaction. Succi's group [7] have adapted the conserved scalar approach and fast-chemistry assumption where reaction is fast in comparison with turbulent mixing processes. This implies that the instantaneous chemical composition of the mixture at a given spatial location is at chemical equilibrium, since the local mixture can be considered isolated and to have enough time to react. With these assumptions, they don't have to solve combustion field directly, and temperature and

concentration fields are determined by one reaction parameter, mixture fraction [8]. This technique is only valid for a non-premixed flame at moderate and high Reynolds number. Succi et al. have simulated a methane/air diffusion flame by simple extension of the Lattice Boltzmann equation to obtain mixture fraction. On the other hand, Filippova et al. has presented a new approach for low Mach number combustion [9]. The flow field is solved by LBM, and transport equations for energy and species are solved by a finite difference scheme. Their model can handle variable density, which is usually important factor in combustion problem. They have focused on diffusion flame formed around a porous cylinder burner. However, they have used artificial mixture and reaction. Also, LB equations and other conservation equations must be coupled in non-dimensional coordinate.

In this study, we will present a lattice Boltzmann model for simulation of combustion. We solve the flow, temperature, and concentration fields using LBM. For simplicity, we assume the chemical reaction does not affect the flow field. Thus, all fields are decoupled and solved separately. The model includes reaction, diffusion, and convection. As a preliminary simulation, we study the so-called "counter-flow" laminar flame. This configuration is considered to occur in turbulent combustion [10-14]. The particular flow geometry is composed of two opposed combustible uniform jets to form a stagnation flow. The twin flames are formed in this counter flow. Since this flame is well understood, it is appropriate for benchmark study. The results are compared with those obtained by conventional scheme from solving Navier-Stokes equations. Also, the counter flame is simulated by compressible Navier-Stokes model to discuss the variable density effect.

MODEL AND ASSUMPTION

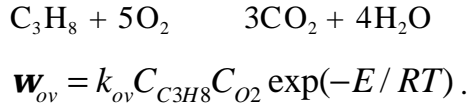
The lattice Boltzmann method has been recognized as an efficient alternative for numerical simulation of fluid flow. For simulation of combustion field, the model includes the reaction term describing heat release and mass rate of production. To

verify the LBM model, we simulate combustion field by the conventional method which consists of conservation equations of mass, momentum, energy, and species. In this section, we explain the flow configurations and assumptions. The governing equations for each method are shown in the next session.

We focus on the counter flow twin flames. Figure 1 shows the schematics of twin flames in counter flow. Two-dimensional rectangular coordinates are used. Two parallel stationary walls are located at $y = -L$ and L , where L is the half-length of the distance between walls. The combustible gas mixture is uniformly ejected from the top and bottom walls, and it reacts in the reaction zone. Then, two flames are formed in this flow. The burned gas flows outward along the x -direction.

The fuel is propane. The following assumptions are made:

1. The flow is symmetric, and there are no external forces.
2. The chemical reaction does not affect the flow field in an incompressible model.
3. The transport properties are constant.
4. The diffusion obeys the Fick's law of diffusion.
5. The reaction is expressed with an over-all one step reaction,



where C_i is the concentration. Mass rate of production for species i is obtained by this over-all reaction rate. The reaction coefficient, k_{ov} , and the effective activation energy, E , are referred to Ref. 14, 15. Nitrogen is assumed to be inert.

6. The heat of formations for the species are adopted from the Joint Army-Navy-Air Force (JANAF) thermochemical tables [16]. The various diffusion coefficients, which are used to evaluate the collision relaxation time, are determined using a rigorous treatment of kinetic theory [17].
7. Viscous energy dissipation and radiative heat loss are neglected.

The half-length of the distance between walls, L , is 10 mm, and longitude length is 16.7 mm. The number of grids is $301(N_x) \times 181(N_y)$, and the mesh size is about 0.05

mm, so as to represent the flame structure accurately. For the stagnation line at $x = 0$ and $y = 0$, we assume the flow is symmetrical. The calculation region is $x \geq 0$ and $y \geq 0$. At the inlet, we adopt inflow boundary. The inlet velocity at the wall, U_0 , in this calculation is 0.2m/s, and Reynolds number is 124. At the outlet, the pressure is constant and we adopt the developed boundary condition.

GOVERNING EQUATION

Lattice Boltzmann Method

We use the incompressible 2D square Lattice BGK model (d2q9) [18]. The relaxation time for flow, temperature, and species are respectively fixed, because transport coefficients, including viscosity, thermal diffusivity, and diffusion coefficient, are constant. We assume the chemical reaction does not affect the flow field for simplicity. Flow, temperature, and concentration fields are decoupled and solved separately. Formula of LBM scheme for flow, temperature, and concentration fields are shown separately as following.

Flow field

The 9-bit lattice BGK model evolves on the two-dimensional square lattice space with the following 9 discrete velocities [18]:

$$\begin{aligned}
 e_0 &= (0, 0) & \alpha &= 0 \\
 e_\alpha &= (\cos[(\alpha-1)\pi/2], \sin[(\alpha-1)\pi/2]) \cdot c & \alpha &= 1, 2, 3, 4 \\
 e_\alpha &= (\cos[(\alpha-5)\pi/2+\pi/4], \sin[(\alpha-5)\pi/2+\pi/4]) \cdot 2 \cdot c & \alpha &= 5, 6, 7, 8
 \end{aligned}$$

where $c = \mathbf{dx}/\mathbf{dt}$, and \mathbf{dx} and \mathbf{dt} are the lattice constant and the time step size, respectively. The evolution equation for an incompressible fluid is

$$p_a(x + e_a \mathbf{d}_i, t + \mathbf{d}_i) - p_a(x, t) = -\frac{1}{\mathbf{t}} [p_a(x, t) - p_a^{eq}(x, t)]$$

$$p_a^{eq} = w_a \left\{ p + p_0 \left[3 \frac{(e_a \cdot u)}{c^2} + \frac{9}{2} \frac{(e_a \cdot u)^2}{c^4} - \frac{3}{2} \frac{u^2}{c^2} \right] \right\}$$

where $t_0 = 4/9$, $t_\alpha = 1/9$ ($\alpha = 1:4$), $t_\alpha = 1/36$ ($\alpha = 5:8$). The sound speed, c_s , is $c/\sqrt{3}$, and $p_0 = \mathbf{r}_0 c_s^2$. The pressure, p , and the velocity, $u = (v_x, v_y)$, are calculated by

$$p = \sum_a p_a$$

$$p_0 u = \sum_a e_a p_a$$

Through the Chapman-Enskog procedure, the incompressible Navier-Stokes equations are derived from these equations. The kinetic viscosity is

$$\mathbf{n} = \frac{2\mathbf{t} - 1}{6} \frac{\mathbf{d}_x^2}{\mathbf{d}_i}$$

Temperature and concentration fields

LBM formula for temperature and concentration fields are as follows:

$$F_{s,a}(x + e_a \mathbf{d}_i, t + \mathbf{d}_i) - F_{s,a}(x, t) = -\frac{1}{\mathbf{t}_T} [F_{s,a}(x, t) - F_{s,a}^{eq}(x, t)] + w_a Q_s$$

$s = T, Y_i$ ($i = \text{C}_3\text{H}_8, \text{O}_2, \text{CO}_2, \text{H}_2\text{O}$).

where

$$F_{s,a}^{eq} = w_a s \left\{ 1 + 3 \frac{(e_a \cdot u)}{c^2} + \frac{9}{2} \frac{(e_a \cdot u)^2}{c^4} - \frac{3}{2} \frac{u^2}{c^2} \right\}$$

The temperature, T , and mass fraction of species i , Y_i , are obtained in terms of the distribution function by

$$T = \sum_{\mathbf{a}} F_{T,\mathbf{a}}$$

$$Y_i = \sum_{\mathbf{a}} F_{Y_i,\mathbf{a}}$$

The source term due to chemical reaction, Q_s , is given by the similarity in non-dimensional equations of temperature and concentration fields. The reaction rate of species i [$\text{kg}/\text{m}^3\text{s}$] appearing in the conservation of species equation is,

$$\mathbf{w}_i = \mathbf{w}_{ov} / M_i = k_{ov} C_{C_3H_8} C_{O_2} \exp(-E / RT) / M_i,$$

where \mathbf{w}_{ov} is the over-all reaction rate [$\text{mol}/\text{m}^3\text{s}$] and M_i is the molecular weight of species i [kg/mol]. The reaction rate is non-dimensionalized by characteristic length, L , velocity, U , and density, ρ . By the similarity in lattice space and real coordinate, the reaction rate in LBM is,

$$(\mathbf{w}_i)_{LBM} = \frac{\mathbf{w}_i}{\rho U / L} \cdot \left(\frac{\mathbf{r}U}{L} \right)_{LBM}.$$

The thermal diffusivity, κ , and diffusion coefficients, D_i , are given by

$$\mathbf{k} = \frac{2\mathbf{t}_T - 1}{6} \frac{\mathbf{d}_x^2}{\mathbf{d}_t}$$

$$D_i = \frac{2\mathbf{t}_{Y_i} - 1}{6} \frac{\mathbf{d}_x^2}{\mathbf{d}_t}$$

Conventional Method

The governing equations of conventional method are based on differential equations maintaining conservation of mass, momentum, energy, and species. These equations describe the convective motion of fluid, the chemical reactions among the constituent species, and the diffusive transport process such as thermal conduction and molecular diffusion. The approach is to solve a set of time-dependent, coupled partial differential equations with a finite difference method [14]. Assuming that the flow quantities are known at a time level t^n , the solution at a new level t^{n+1} is obtained by using the Crank-Nicholson method. This procedure is continued until a steady solution is obtained. The algebraic equations yielded from discretization are solved by the Gauss-Seidel method.

Stream function and axial and radial velocities

$$u = \frac{d\mathbf{j}}{dy}, \quad v = -\frac{d\mathbf{j}}{dx}$$

where φ is the stream function to satisfy the conservation of mass (overall continuity equation).

Vorticity equation

$$\frac{dW}{dt} + u \frac{dW}{dx} + v \frac{dW}{dy} = \mathbf{n} \left\{ \frac{d^2W}{dx^2} + \frac{d^2W}{dy^2} \right\},$$

$$W = \frac{dv}{dx} - \frac{du}{dy} = - \left\{ \frac{d^2\mathbf{j}}{dx^2} + \frac{d^2\mathbf{j}}{dy^2} \right\},$$

where W [1/s] is the vorticity.

Energy equation

$$\frac{dT}{dt} + u \frac{dT}{dx} + v \frac{dT}{dy} = \kappa \left\{ \frac{d^2T}{dx^2} + \frac{d^2T}{dy^2} \right\} + \frac{Q \cdot \mathbf{w}_{ov}}{\mathbf{r} \cdot C_p},$$

where Q [J/mol] is the heat of overall reaction, C_p [J/kgK] is the heat capacity, and κ [m²/s] is the thermal diffusivity.

Species conservation

$$\frac{dY_i}{dt} + u \frac{dY_i}{dx} + v \frac{dY_i}{dy} = \frac{D_i}{\mathbf{r}} \left\{ \frac{d^2Y_i}{dx^2} + \frac{d^2Y_i}{dy^2} \right\} + \frac{\omega_i}{\mathbf{r}}, \quad i = \text{C}_3\text{H}_8, \text{O}_2, \text{CO}_2, \text{H}_2\text{O},$$

where ω_i [kg/ m³s] is the reaction rate of species i , and D_i is the diffusion coefficient. Since nitrogen is taken as inert, its mass fraction is obtained by

$$Y_{N_2} = 1 - \sum_{i \neq N_2} Y_i.$$

Equation of state

In an incompressible model, we use the following equation of state for the mixture.

$$\mathbf{r} = p / \left\{ R_u T \sum_i (Y_i / M_i) \right\},$$

where R_u is the universal gas constant (8.315 J/mol·K). The static pressure is obtained by solving the Poisson- equation of pressure derived using the conservation of momentum.

Equivalence Ratio

The equivalence ratio is defined as the ratio of the actual fuel-oxidant mass ratio to the ratio $(F/O)_{st}$ for a stoichiometric process [8]. The stoichiometric reaction is defined as a unique reaction in which all the reactants are consumed. When the fuel is propane, the stoichiometric process is $\text{C}_3\text{H}_8 + 5\text{O}_2 \rightarrow 3\text{CO}_2 + 4\text{H}_2\text{O}$, and the equivalence ratio by using mass fraction of propane and oxygen, ϕ , is

$$\mathbf{f} = \frac{(F/O)}{(F/O)_{st}} = \frac{Y_F/Y_O}{(44.1)/(5 \times 32.0)} = \frac{Y_F/Y_O}{0.276},$$

where the molecular weights of propane and oxygen are 44.1 and 32.0 g/mol. For fuel-lean conditions, we have $0 < \phi < 1$, for stoichiometric conditions, we have $\phi = 1$, and for fuel-rich conditions, we have $1 < \phi < \infty$. In this calculation, the mixture is lean propane/air.

RESULTS AND DISCUSSION

Flow field

First, we examine the flow field where counter flames are formed. We compare the results from both the Lattice Boltzmann method and a conventional method. Figure 2 shows the distribution of velocities of v_x at $y = 0$ and v_y at $x = 0$, respectively. The velocity is normalized to the inlet velocity at the wall, U_0 . Both results show good agreement, though the LBM v_x is slightly higher. This may be caused by the slip boundary condition at $y = 0$ in LBM calculation, which differs to the symmetric condition adopted in conventional simulation. The flow field is well simulated in the case of counter flow.

Temperature and concentration field

Next, we investigate the temperature and concentration fields. Before that, we calculate the combustion field in simple flow to confirm that reaction scheme is well described. We simulate the flame formed in uniform flow. The number of grid points is $501(N_x) \times 3(N_y)$. We calculate the flame motion using d2q9 LB model. Both the upper and lower boundaries have free slip boundary conditions. The flame shows 1-D behavior, so that it is easy to analyze the flame motion. Figure 3 shows the

contour of the overall reaction rate. The equivalence ratio, ϕ , is 0.6. The inlet velocity, U_{in} , is 1 m/s in the real coordinate, and $(U_{in})_{LBM}$ is 0.1. The inlet position is at the left edge of the profile. It is seen that the flame is moved downstream. This is because the flow velocity is much larger than the burning velocity, S_L , which is defined by the flow velocity if the flame is stationary [8]. Then, we try to obtain the burning velocity in this calculation.

Figure 4 shows the flame position in lattice space where the reaction rate reaches its maximum. Its initial position is $IY = 50$, and it moves downwards. Since its flame speed, V_f , is equal to the inlet velocity subtracted by the burning velocity, $S_L = U_{in} - V_f$, the burning velocity can be estimated. Using the relation between lattice space and real coordinate, the burning velocity is obtained by the following equation,

$$S_L = \left(\frac{S_L}{U_{in}} \right)_{LBM} \cdot U_{in} = \left(\frac{U_{in} - V_f}{U_{in}} \right)_{LBM} \cdot U_{in}.$$

The resultant burning velocity in Fig. 4 is 0.12 m/s. The experimentally obtained burning velocity is 0.11 m/s [19]. The difference may be caused by the simple assumption of one step reaction. It appears that the reaction term is well described in this calculation.

Next, we show some results of the counter-flow flame. Figure 5 shows the temperature contour and the velocity vectors. The unburned gas at room temperature, 300K, is ejected from the porous wall, and reacts in the flame zone, and finally it becomes burned gas. The temperature is almost constant along the x-axis. The profiles along the center, $x = 0$ is shown. Figure 6 shows the temperature and concentration distributions. The over-all reaction rate, which is equal to the molar fuel consumption rate, is also shown. As seen in Fig. 6(a), as the center is approached, the temperature starts to increase at $y \cong 3$ mm, and steeply increases at $y = 2 - 3$ mm. As seen in the reaction rate profile, the reaction zone is located in this

region, where the large heat release occurs causing the temperature rise. Beyond that, temperature becomes constant in the burned gas region.

Figure 6(b) shows the mass fraction profile. As seen in this figure, the reactant, C_3H_8 and O_2 , begins decreasing at the edge of preheat zone ($r \cong 3$ mm), and reacts in the reaction zone to form the product, CO_2 and H_2O . The fine structure of counter flow flame is observed.

Then, we compare results by LBM and conventional method. The distribution of temperature and reaction rate is shown in Fig. 7. From this figure, we see that the two profiles are perfectly matched and we confirm that the reaction scheme in LBM is capable of calculating the combustion field.

Flame Temperature

Next, we change the fuel concentration and examine the flame temperature, which is an important feature of the flame. As seen in the temperature distribution in Figs. 5 and 6, the maximum temperature is located at the center line ($y = 0$ mm) and is almost constant. Then, we define this maximum temperature as flame temperature, T_f . We compare the flame temperatures obtained by two different schemes. To examine the effect of compressibility, we also solve the compressible Navier-Stokes equations.

Figure 8 shows the variations of the flame temperature, T_f , with equivalence ratio. From this figure, it is seen that the flame temperature monotonically increases with increasing equivalence ratio. This is because the deficient reactant is fuel and the combustion is intensified by increasing the fuel concentration. When we compare the temperatures obtained by LBM and incompressible FDM, both results are almost the same. If we take the variable density into account, the calculated flame temperature is slightly decreased. If the density is changed, the velocity is changed and this affects the temperature field. Although it is expected that this temperature is more close to the real temperature, many factors including detailed chemistry, the

variable transport coefficients, and radiation effect are still needed to simulate the exact flame temperature [20]. In the present, we conclude that, as an alternative approach, Lattice Boltzmann method can be used to simulate combustion field.

CONCLUSIONS

In this present paper, we have proposed the numerical procedure for simulating a combustion flow using an incompressible LB model. We have focused on laminar flame formed in counter flow as a benchmark study. We assume the chemical reaction does not affect the flow field for simplicity. We use a propane-air premixed mixture with a one-step Arrhenius-type reaction model. To verify our LBM model, we solve the governing equations for conservation of mass, momentum, energy, and species by finite difference method. The results of both simulations are in good agreement. If we take the variable density into account, the calculated flame temperature is slightly decreased. Although some improvement may be needed, it is concluded that, the LBM approach can be used to simulate combustion.

REFERENCES

1. Williams, F. A., *Combustion Theory*, Benjamin Cummings, Redwood City, 1985.
2. Peters, N., *Twenty-First Symposium (International) Combustion*, The Combustion Institute, Pittsburgh, 1986, pp. 1231-1250.
3. Chen, S. and Doolen, G. D., *Annual Reviews of Fluid Mech.*, 1998, pp.329-364.
4. He, X. and Doolen, G. D., *Physical Review E* 56-1, 1997, pp. 434-440.
5. Martinez, D. O., Matthaeus, W. H., Chen, S., and Montgomery, D. C., *Phys. Fluids* 6, 1994, pp. 1285-1298.
6. Chen, S., Martinez, D. O., Mei, R., *Phys. Fluids* 8, 1996, pp. 2527-2536.

7. Succi, S., Bella, G., and Papetti, F., *J. Scientific Computing Vol. 12-4*, 1997, pp. 395-408.
8. Kuo, K. K., *Principles of Combustion*, John Wiley and Sons, New York, 1954.
9. Filippova, O., and Hanel, D., *J. Computational Physics*, 158, 2000, pp.139-160.
10. Tsuji, H. and Yamaoka, I., *Nineteenth Symposium (International) Combustion*, The Combustion Institute, Pittsburgh, 1982, pp. 1533-1540.
11. Ishizuka, S., and Law, C. K., *Nineteenth Symposium (International) Combustion*, The Combustion Institute, Pittsburgh, 1982, pp. 1541-1548.
12. Smooke, M. D., and Giovangigli, V., *Lecture Notes in Physics 241*, Springer-Verlag, 1985, pp.1-28.
13. Libby, P. A., Peters, N., and Williams, F. A., *Combust. Flame* **75** (1989), pp. 265- 280.
14. Yamamoto, K., *Combust. Flame* **118** (1999), pp. 431-444.
15. Westbrook, C. K. and Dryer, F. L., *Combust. Sci. Technol.* 27, 1981, pp. 31-43.
16. Stull, D. R. and Prophet, H., *JANAF Thermodynamic Tables*, NSRDS-NBS **37**, National Bureau of Standards, Washington, D. C., 1971.
17. Hirshfelder, J. O., Curtis, C. F., and Bird, R. B., *Molecular Theory of Gases and Liquids*, John Wiley and Sons, New York, 1954.
18. He, X. and Luo Li-Shi, *J. Statistical Physics*, Vol. 88, Nos. 3/4, 1997, pp. 927-944.
19. Yamaoka, I. and Tsuji, H., *Twentieth Symposium (International) Combustion*, The Combustion Institute, Pittsburgh, 1982, pp. 1883-1892.
20. Ju, Y., Masuya, G., Liu, F., Guo, H., Maruta, K., and Niioka, T., *Twenty-Seventh Symposium (International) Combustion*, The Combustion Institute, Pittsburgh, 1998, pp. 2551-2557.

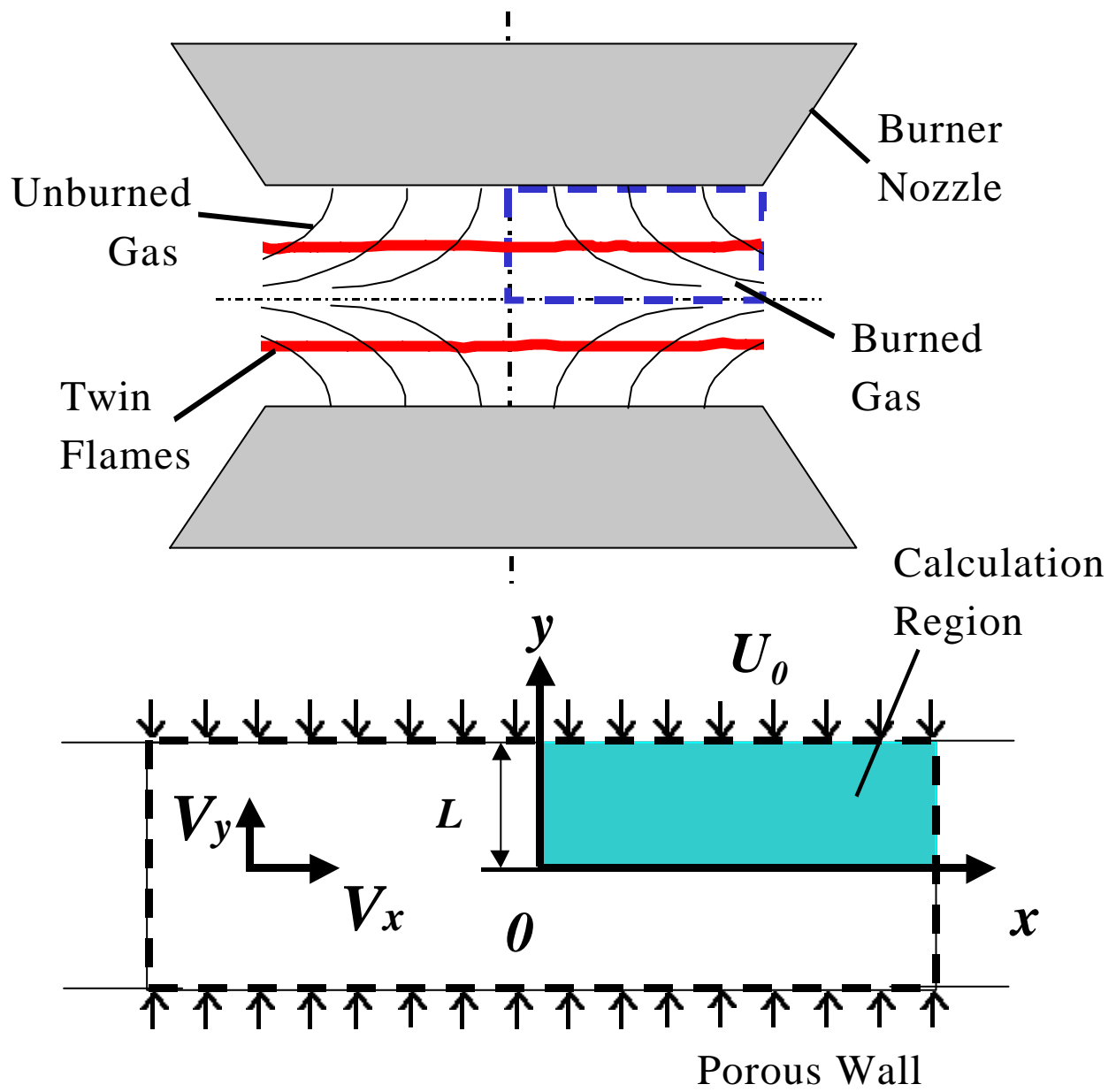


Fig. 1. Counter flow and coordinate.

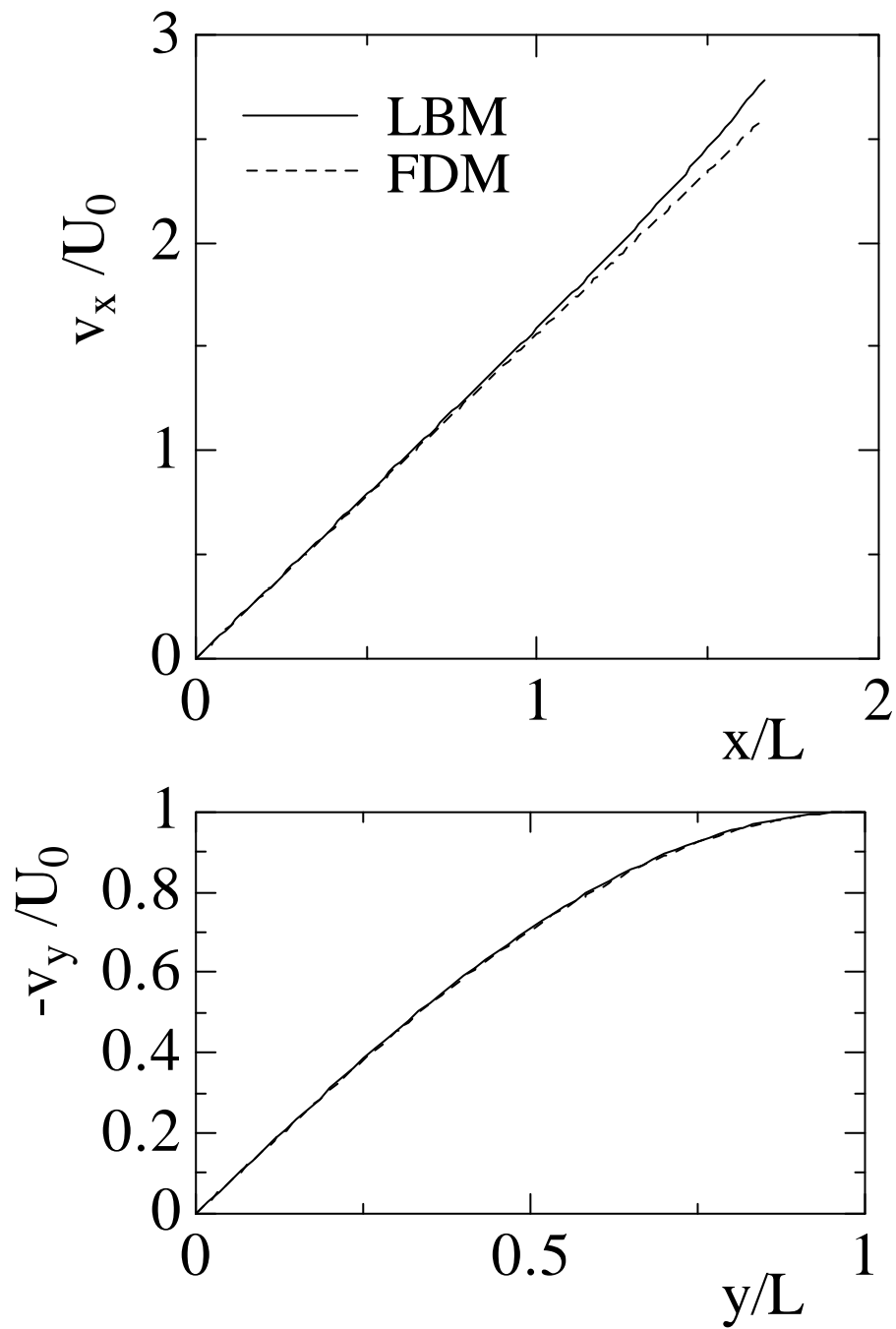


Fig. 2. Distribution of non-dimensional velocity of v_x and v_y ; $Re=124$.

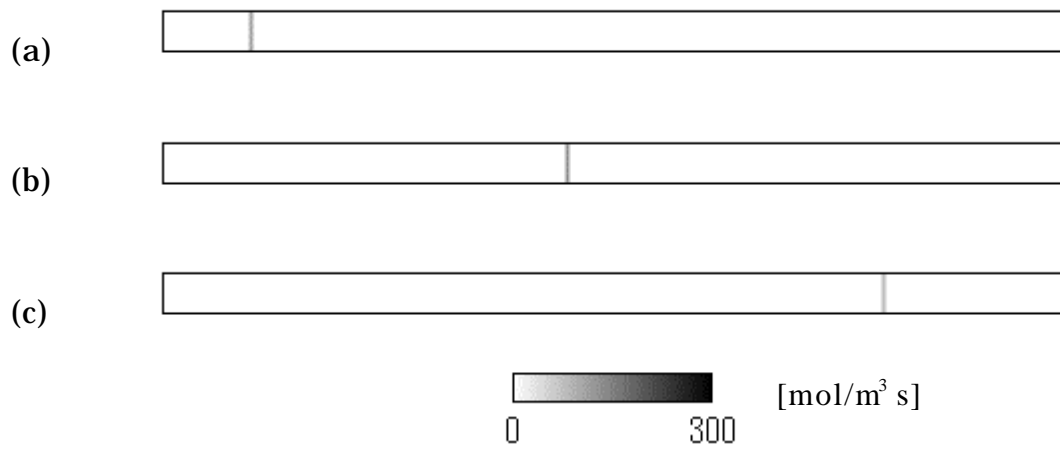


Fig. 3. Contour of reaction rate of a flame formed in uniform flow; (a) $t = 0$, (b) $t = 2000$, and (c) $t = 4000$.

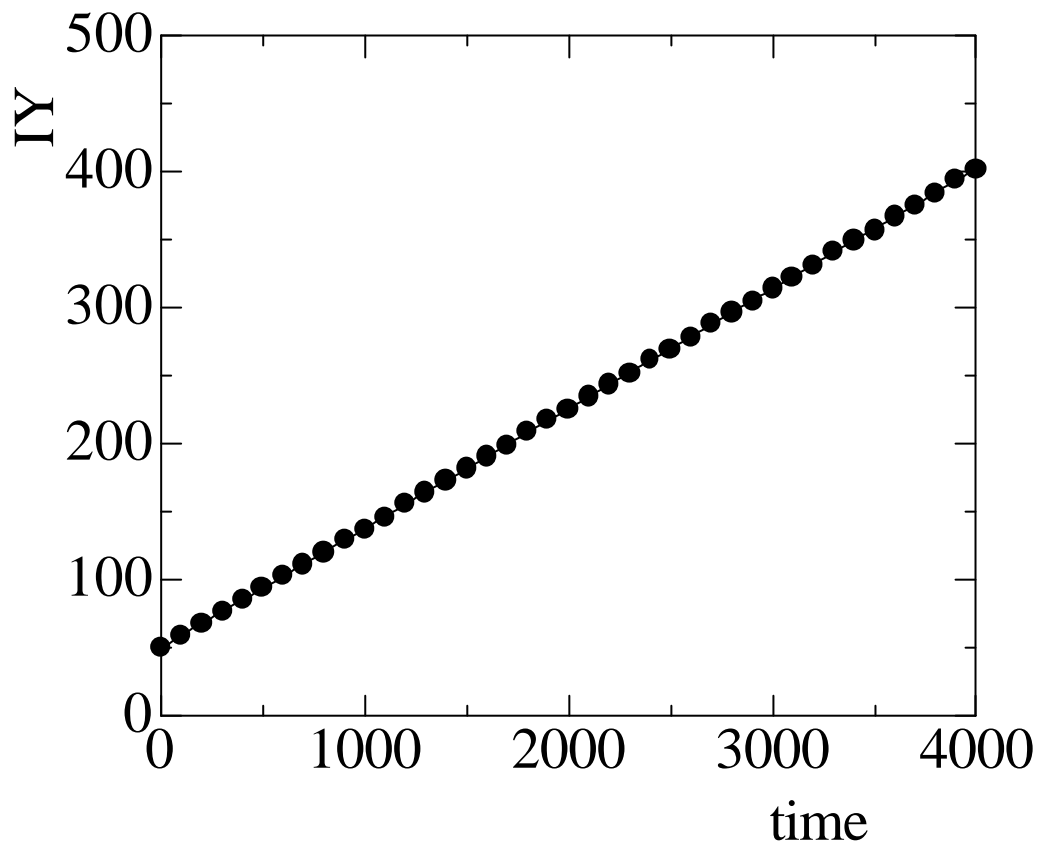


Fig. 4. Position of reaction zone, $U_{in}=0.1$,
 $=0.6$.

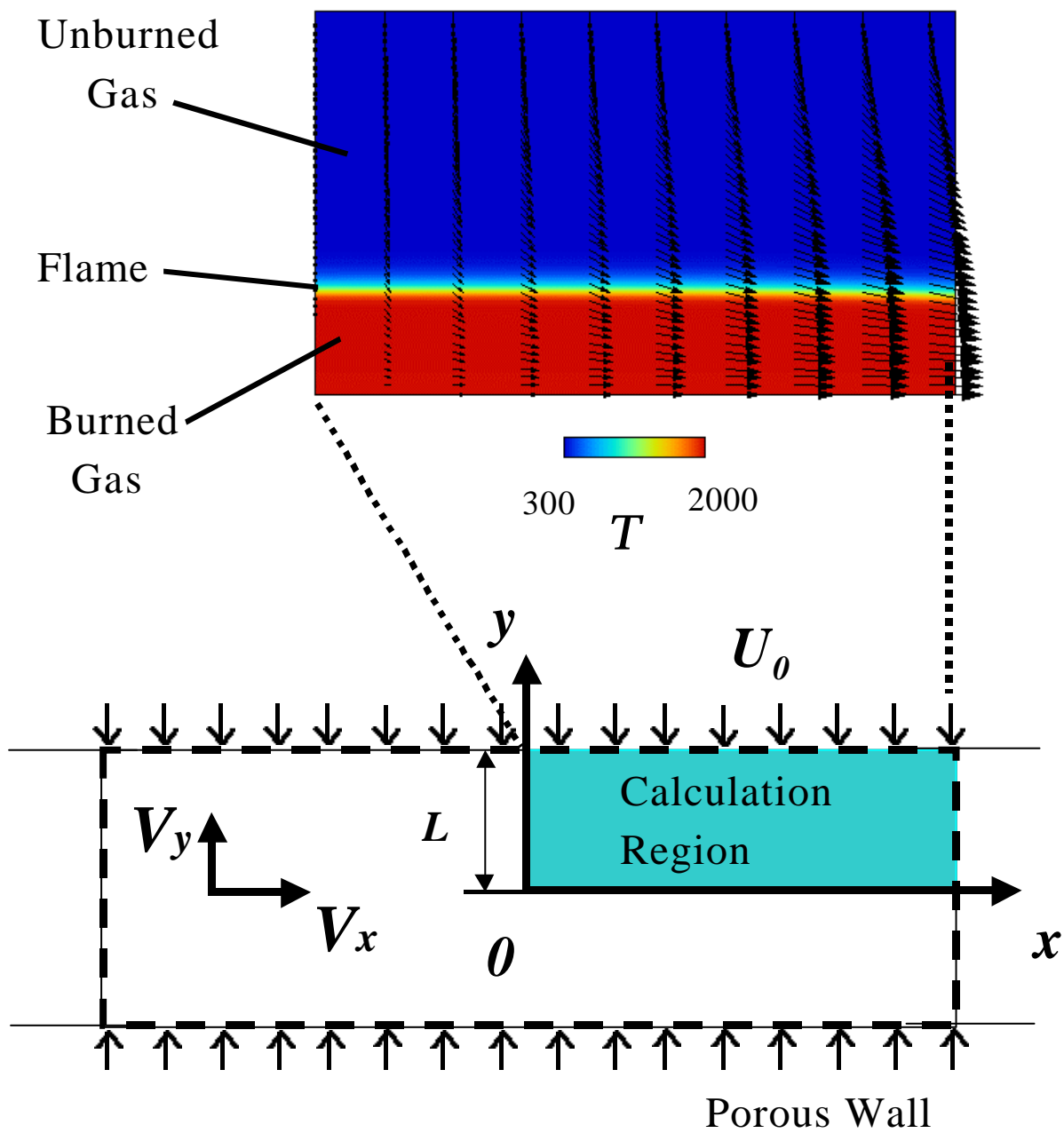


Fig. 5. Temperature profile.

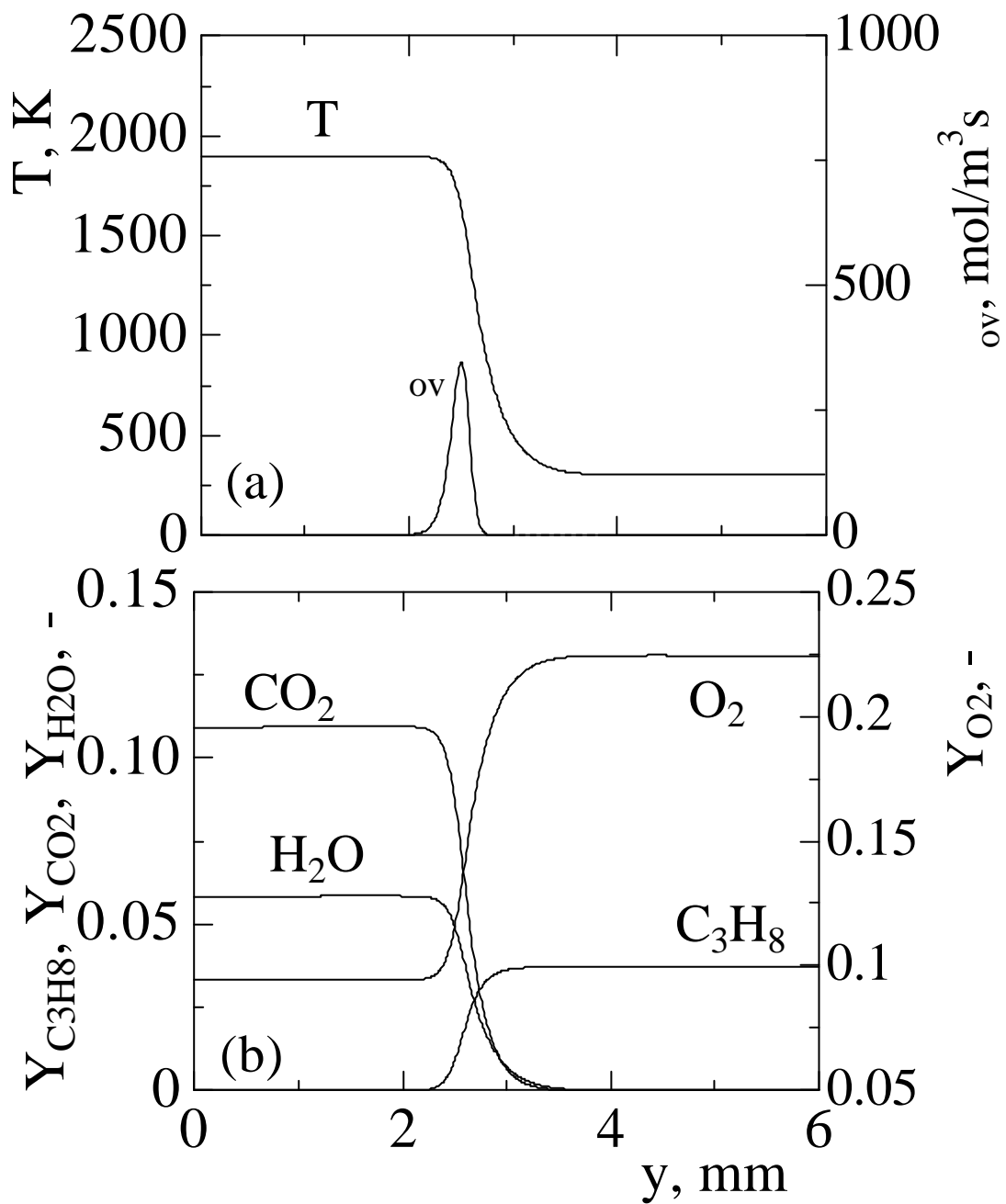


Fig. 6. Distributions of (a) temperature and reaction rate, (b) mass fraction of species; $\phi = 0.6$, $Re=124$.

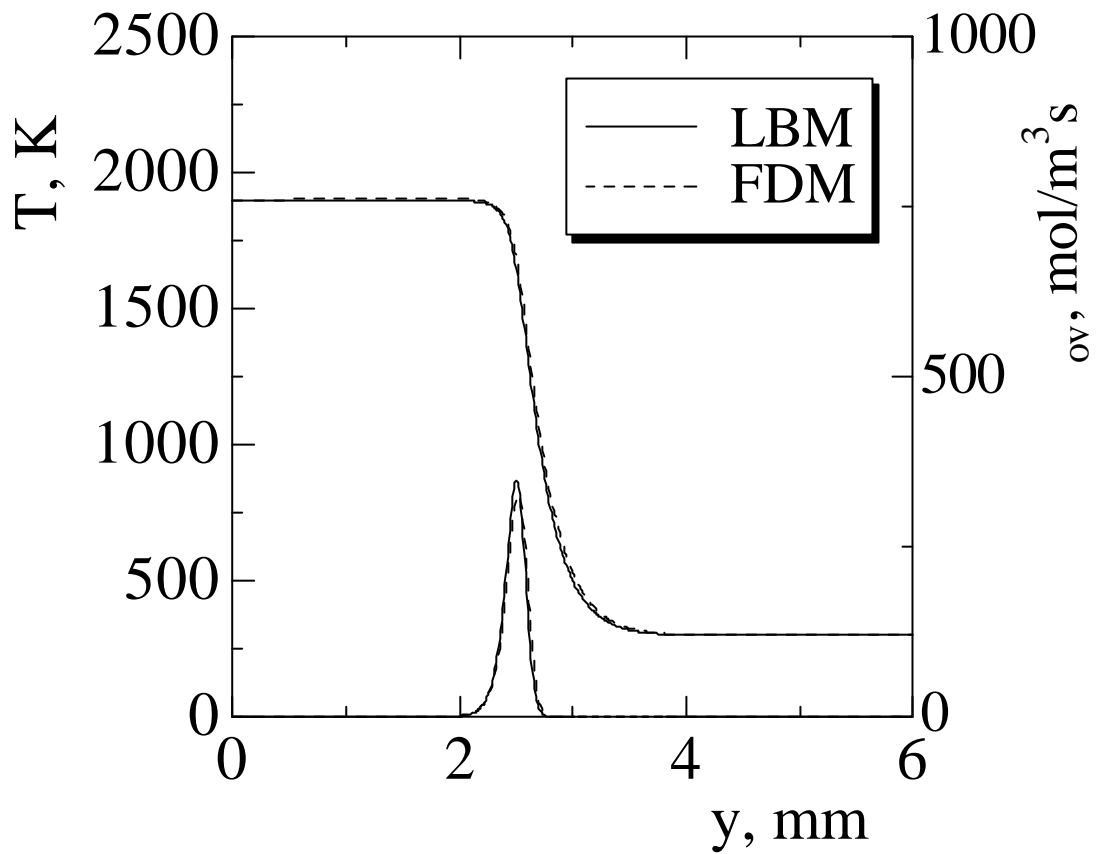


Fig. 7. Distribution of temperature and reaction rate; $\phi = 0.6$, $Re = 124$.

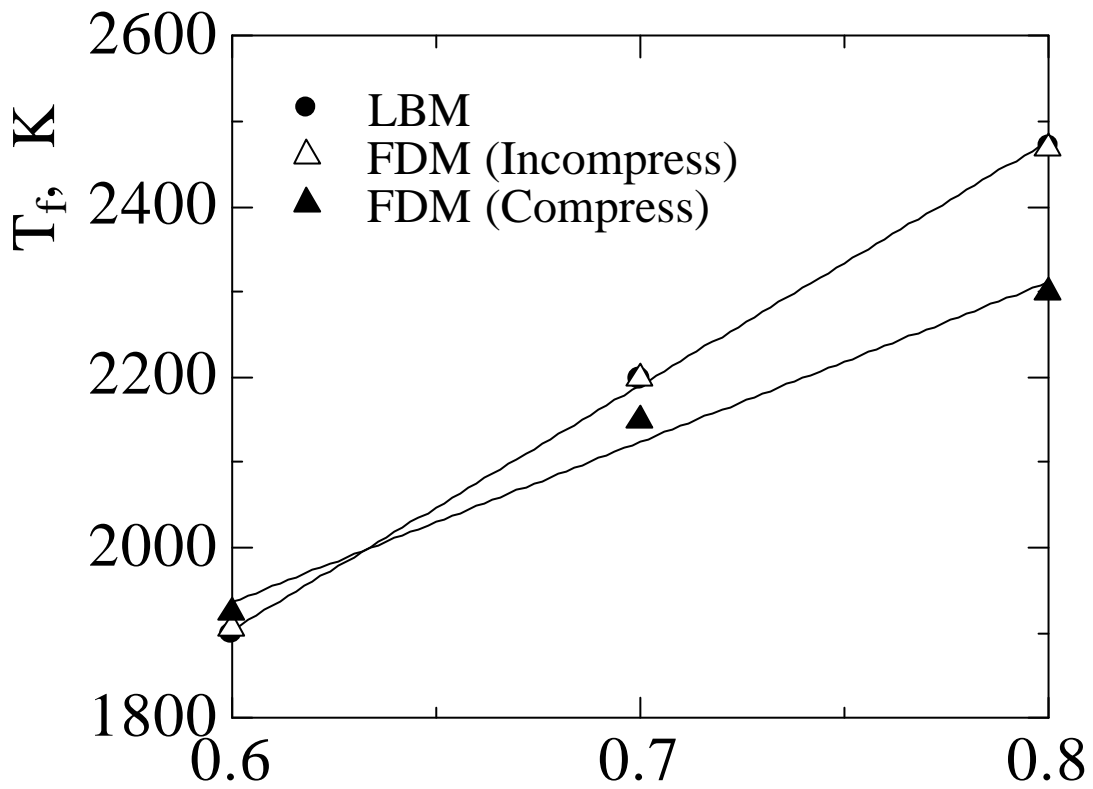


Fig. 8. Variations of flame temperature with equivalence ratio for propane/air mixtures.